Ionization of multielectron atoms using Slater-type wave functions

S. Sahoo, R. Das, N. C. Sil, S. C. Mukherjee, and K. Roy
Department of Theoretical Physics, Indian Association for the Cultivation of Science, Jadavpur, Calcutta 700032, India
(Received 7 September 1999; published 20 July 2000)

The single ionization of multielectron atoms by the impact of protons, antiprotons, and highly charged bare ions is studied. The targets are treated as one-electron atoms, where the interaction of the active electron with the rest of the target is represented by a model potential. The final electronic state is described by the product of two Coulomb wave functions that put the distortion due to the projectile and the target on equal footing. We calculate the total and differential ionization cross sections for helium- and lithium-atom targets. The results thus obtained are compared with existing experimental data and other available theoretical predictions.

PACS number(s): 34.50.Fa

I. INTRODUCTION

In recent years there have been ongoing attempts to study both theoretically and experimentally collision processes such as charge transfer, ionization, and excitation resulting from the impact of multicharged ions on multielectron target atoms. In the case of charge transfer and excitation, the target electron remains bound to either the target or the projectile. This situation makes the electron dynamics somewhat simpler. For the ionization of atoms, the complication arises that the electron in the final state moves under the combined influences of the projectile and the residual target. So one has to solve at least a three-body problem in which three particles interact via Coulomb potentials. Due to the long-range nature of the Coulomb potential, the free electronic state cannot be represented by only a plane wave. An exact solution for the problem is difficult to obtain; however, its correct asymptotic form is available (cf. [1,2]).

Ionization by charged-particle impact can be traced back to 1912, when J. J. Thompson suggested a classical model of the problem in which the electron in the atom is treated to be at rest and it is assumed that ionization has occurred if the projectile has transferred an amount of energy greater than the ionization potential to the target atom. The problem was treated quantum mechanically in the 1930s (cf. Bethe [3] and Massey and Mohr [4]), and later was understood from the pioneering work of Bates and Griffing [5], in which the first Born approximation (FBA) was used to study both the ionization and excitation of hydrogen atoms. In this model, the initial bound-state wave function is undistorted and the final-state wave function considers the electron to move under the Coulomb potential centered on the target atom. As the FBA is a correct first-order theory, it predicts total ionization cross sections (TIC's) in the high-energy region accurately. However, it is still not free from ambiguity and fails to describe all the features in the electron ejection spectra. As the electron in the final state moves under the influence of two Coulomb potentials, the electron ejection spectra show different features, such as the soft collision peak, electron capture to the continuum peak, and the binary encounter peak. These structures show a very different dependence on collision parameters, such as the projectile charge or velocity. Therefore a complete and accurate description of emission spectra is of great theoretical interest. Recently, Stolterfoht *et al.* [6] have published a book about the physics of the above process and summarized it both theoretically and experimentally.

Although the simplest target is atomic hydrogen, almost all experiments are carried out with the multielectron targets. For hydrogen-atom targets, many theoretical and experimental studies have been done in an attempt to understand the mechanism of ionization. Schultz *et al.* [7] studied electron ejected spectra for proton-atomic hydrogen (p-H) collisions both experimentally and theoretically, applying the classical trajectory Monte Carlo (CTMC) method. The continuum distorted-wave–eikonal initial-state (CDW-EIS) model, which has been introduced by Crothers and McCann [8], is found to be successful in predicting the total and differential ionization cross sections in intermediate to high energy collisions. Different features in the electron spectra are described by many authors applying this model. Sahoo *et al.* [9] have applied the perturbative approach to study proton impact ionization of atoms under heavy particle impact, in which the continuum-state wave function is represented by the product of two Coulomb waves and thus the ejected electron is considered to be moving under the combined influence of the projectile and the residual target. They have reported a number of interesting features in the electron ejected spectra for p-H ionization.

The development of ion sources producing multiply charged ions and antiproton beams has presented a challenge for theoretical physicists. Toshima [10] studied the ionization of atomic hydrogen by the impact of multiply charged bare ions, applying a close-coupling method. Recently, Sahoo *et al.* [11] have also investigated the ionization of hydrogen atoms by fully stripped ion impact at high energies.

Presently, there are vast amounts of experimental data available for the single ionization of multielectron targets, but no theoretical result agrees quantitatively with the experimental data over the whole angular and energy range. The single ionization by impact of multicharged ions has been studied by Fainstien *et al.* [12] within the framework of CDW-EIS. McCartney and Crothers [13] approached this model with a slightly different perspective by studying the single ionization of lithium, beryllium, and neon by ion impact. They represented the initial bound-state wave function using Roothan-Hartree-Fock (RHF) wave functions [14]. To stay within the context of the CDW-EIS, they approximated the ionized-electron-residual-target interaction by a Coulombic potential, assuming that the ejected electron is ionized from an orbital of RHF energy and moves in the residual

potential. Continuum states were described by hydrogenic wave functions with an effective charge chosen from the energy of the initial bound state [12]. In doing so, the initial and final states correspond to different potentials and thus they are not orthogonal. The nonorthogonality leads to an underestimation of the cross section as explained by Gulyas *et al.* [15]. The results obtained by these authors are found to underestimate slightly the experimental data for the ionization of Li($1s$) by proton and α-particle impact. For the case of proton impact on Ne, they obtained very good agreement with the experimental data of Rudd *et al.* [16]. However, the present approach uses a model potential, which consists of both short- and long-range parts. The bound-state wave functions are obtained from the model potential. The initial bound and final continuum states are described by an asymptotic charge instead of an effective charge, as has been chosen in Ref. [13].

It is well known from the work of Madison [17] that the theoretical models for ionization are sensitive to the quality of the target wave function. As such, it is of current interest to describe the target wave function more accurately. In 1995, Gulyas *et al.* [15] generalized the CDW-EIS model for ion impact on multielectron targets where the interaction of the active electron with the target was represented by a Hartree-Fock potential. They numerically calculated both the initial bound state and final continuum state of the target atoms by solving the time-independent Schrödinger equation with a model potential and obtained better results than predicted by the previous CDW-EIS model of Ref. [13]. However, their calculated values are too high in the region of the maximum in the experimental data of Shah and Gilbody [18] and Shah *et al.* [19] for helium-atom targets. For the ionization of Ar by proton impact, Gulyas *et al.* [15] obtained higher values than the experimental data of Rudd *et al.* [16], and in the case of ionization of Ne by proton impact, they found that their results reproduce the experimental data more accurately in the high-energy range. However, better results are obtained at the expense of a greater computational effort.

In 1998, Gulyas and Fainstein [20] generalized the CDW model for single ionization of multielectron atoms by ion impact, where the interaction of the active electron with the target was described by a model potential. Their work is closely related to the work of Gulyas *et al.* [15]. In this work, the significant difference in the initial-state wave function between the CDW-EIS [15] and CDW (Ref. [21]) is that the former accounts for the distortion as an eikonal phase factor and the latter uses a continuum factor. This phase corresponds to the asymptotic behavior of the continuum factor at large distances. The CDW model with the continuum factor largely overestimates the cross sections at intermediate energies.

In the present article, we have calculated the ionization cross sections of helium and lithium atoms by the impact of protons, antiprotons, and multiply charged bare ions. We describe the multielectron targets as having only one active electron that moves under the influence of an effective potential due to the target core and passive electron(s).

II. THEORY

To study the ionization process of multielectron targets in the high-energy region, we apply the theory described by Sahoo *et al.* [9], which has already been successfully applied by them to the ionization of hydrogen by the impact of protons, antiprotons, and fully stripped ions. The collision system under study is a complex one due to the presence of more than one electron in the target atom. In order to simplify it, we have treated the multielectronic targets as having only one active electron, which experiences an effective potential due to the target nucleus and the passive electron(s). We solve the one-electron Schrödinger equation for the system with electronic Hamiltonian

$$\mathrm{H}_e = -\frac{1}{2}\nabla_r^2 + V_T(r_T) + V_P(r_P) \tag{1}$$

(atomic units are used throughout), where $r_P(r_T)$ is the distance of the electron from the projectile (target). We adopt here the impact-parameter formalism, where the internuclear motion is treated classically as $\vec{R}=\vec{p}+\vec{v}t$, in which $\vec{p}$ is the impact parameter, $\vec{v}$ is the relative velocity of the projectile with the target, and the midpoint of the line joining the two nuclei is chosen as the origin. Time is measured from the instant when the two nuclei are the closest to each other.

The development in time t of the transition amplitude for ionization with the ejection of an electron with momentum $\vec{k}$ can be written as

$$\frac{d}{dt}(c_k(p)) = \int \left[\psi_{k_c}^{-*} \left(H_e - i\frac{d}{dt} \right) \Psi_i^+ \right] d\vec{r}, \tag{2}$$

with the initial condition that at $t=-\infty$, $c_k=0$. The ionization probability is $|c_k(t=+\infty)|^2$.

The continuum-state wave function is represented by the product of two Coulomb wave functions, where the residual target core is assumed to be Coulombic. This assumption is valid for high velocities of the projectile ion. The wave function in the final channel is of the form

$$\psi_{k_c}^- = N_1 N_2 e^{i\vec{k}\cdot\vec{r}} {}_1F_1(i\alpha_p,1;-i(k_p r_p + \vec{k}_p\cdot\vec{r}_p)) \times {}_1F_1(i\alpha_T,1;-i(k_T r_T + \vec{k}_T\cdot\vec{r}_T)) e^{-ik^2 t/2}, \tag{3}$$

where $\alpha_P=-Z_P/k_P$, $\alpha_T=-q_T/k_T$, $\vec{k}_P=\vec{k}-\vec{v}/2$, $\vec{k}_T=\vec{k}+\vec{v}/2$, and

$$N_1 = e^{-\pi\alpha_P/2}\Gamma(1+i\alpha_P),\quad N_2 = e^{-\pi\alpha_T/2}\Gamma(1+i\alpha_T);$$

Z_p is the nuclear charge of the projectile and q_T is the asymptotic charge of the target ion.

The above continuum-state wave function asymptotically satisfies the Schrödinger equation,

$$\left(-\frac{1}{2}\nabla_r^2 - \frac{Z_P}{r_P} - \frac{q_T}{r_T} - i\frac{\partial}{\partial t} \right) \psi_{k_c}^- = 0. \tag{4}$$

A. Construction of an initial bound-state wave function

The interaction of one active electron and the residual target ion of asymptotic charge q_T may be described in different ways. We have used a model potential of the form

$$V_T = -\frac{q_T}{r_T} - \frac{\exp(-\lambda r_T)}{r_T}\{(Z-q_T)+br_T\}, \tag{5}$$

where Z is the nuclear charge of the target ion. b and λ are parameters determined variationally with respect to the Slater basis set in such a way that the corresponding Hamiltonian of the active electron is diagonalized to reproduce the correct binding energies. These binding energies of the active electron on different target ions are calculated from the tables of Clementi and Roetti [14]. To check the accuracy of the wave function, the virial theorem has been tested, and it is found to be accurate within 0.01%. The present model potential is similar to the potentials used by Ermolaev *et al.* [22] and Ermolaev [23] in the studies of charge-transfer processes involving lithium and cesium targets and also those used by Shingal *et al.* [24] in the study of charge transfer in proton-sodium collisions.

The initial-state wave function used in the present approach can be written as

$$\Psi_i^+ = \phi_i(r_T)\exp\left(-\frac{i}{2}\vec{v}\cdot\vec{r}\right)\exp\left(-i\varepsilon-\frac{i}{8}v^2\right)t, \tag{6}$$

where

$$\phi_i(r_T) = \sum_j c_j^{nl} e^{-\beta_j r_T} r_T^l Y_{lm}(\hat{r}_T).$$

c_j and β_j are the coefficients and the exponents of the Slater orbitals.

B. Transition amplitude

Following the work of the present authors [9], we derive the transition amplitude as follows: Using Eqs. (3), (4), and (6) and then the contour integral representations of confluent hypergeometric functions [25], we may write Eq. (2) as

$$\begin{aligned} c_k(p) = A_k \oint_{\Gamma_1}\oint_{\Gamma_2} dt_1 dt_2 t_1^{-i\alpha_p-1}(t_1-1)^{i\alpha_p} t_2^{-i\alpha_T-1} \\ \times (t_2-1)^{i\alpha_T}\int e^{iEt}dt \int e^{-i\vec{K}\cdot\vec{r}} \\ \times\left(\frac{c_1 e^{-\beta_1 r_T}+\cdots+c_n e^{-\beta_n r_T}}{r_p}\right) \\ \times (e^{it_1 k_p r_p + it_2 k_T r_T} e^{it_1\vec{k}_p\cdot\vec{r}_p + it_2\vec{k}_T\cdot\vec{r}_T}) d\vec{r}, \end{aligned} \tag{7}$$

where $\vec{K}=\vec{k}+\vec{v}/2$, $E=(k^2/2-v^2/8-\epsilon)$, and $A_k = (N_1^* N_2^*)/(4\pi^{5/2})$.

As the bound-state wave function is a linear combination of Slater-type orbitals (STO's), the integral in Eq. (7) can be expressed as a sum of several independent integrals. Here we illustrate the evaluation of one such integral, which may be written as

$$\begin{aligned} I = \lim_{\eta_1\to 0}\int \oint_{\Gamma_1}\oint_{\Gamma_2} e^{-i\vec{K}\cdot\vec{r}-\beta r_T-\eta r_p}\left(\frac{1}{r_p}\right) e^{i(t_1\vec{k}_p\cdot\vec{r}_p + t_2\vec{k}_T\cdot\vec{r}_T)} \\ \times t_1^{-1-i\alpha_p}(t_1-1)^{i\alpha_p} t_2^{-I-i\alpha_T}(t_2-1)^{i\alpha_T} dt_1 dt_2 d\vec{r}, \end{aligned} \tag{8}$$

where $\beta=\beta_1-it_2k_T$ and $\eta=\eta_1-it_1k_p$.

To deduce the integration in Eq. (8), we have to evaluate the following integral:

$$J = \int \frac{e^{-i\vec{K}\cdot\vec{r}-\beta r_T-\eta r_p}}{r_p r_T} e^{i(t_1\vec{k}_p\cdot\vec{r}_p + t_2\vec{k}_T\cdot\vec{r}_T)} d\vec{r}.$$

Using the Fourier transformation technique, we can write

$$J = \frac{2}{\pi}\int \frac{e^{i\vec{Q}\cdot\vec{R}}}{(A-Bt_1)(C-Dt_2)} d\vec{Q}, \tag{9}$$

where $A=(\vec{Q}-\vec{K}/2)^2$, $B=\vec{k}_p\cdot(\vec{K}-2\vec{Q})$, $C=(\vec{Q}+\vec{K}/2)^2+\beta^2$, and $D=\vec{k}_T\cdot(2\vec{Q}+\vec{K})+2i\beta k_T$. Performing the contour integrations over t_1 and t_2 we get Eq. (8) as

$$\begin{aligned} I = [(2\pi i)^2/\pi]\lim_{\eta_1\to 0}\frac{\partial}{\partial\beta}\Bigg[\int_{-\infty}^{+\infty}\exp[i(E+\vec{Q}\cdot\vec{v})t]dt \\ \times\int \exp(i\vec{Q}\cdot\vec{p})A^{-1-i\alpha_p}\times(A-B)^{i\alpha_p} \\ \times C^{-1-i\alpha_T}(C-D)^{i\alpha_T} d\vec{Q}\Bigg]. \end{aligned} \tag{10}$$

Evaluating the time integral, we are left with

$$\begin{aligned} I = [(2\pi i)^2(4)]\Bigg[\int \delta(E+\vec{Q}\cdot\vec{v})\exp(i\vec{Q}\cdot\vec{p})A^{-1-i\alpha_p} \\ \times(A-B)^{i\alpha_p} C^{-1-i\alpha_T}(C-D)^{i\alpha_T} d\vec{Q}\Bigg]. \end{aligned} \tag{11}$$

To simplify the integration over $\vec{Q}$, let us consider the z axis along the direction of $\vec{v}$, then the three-dimensional vectors can be represented in the following manner: $\vec{Q}=\vec{Q}_z+\vec{\rho}$, $\vec{k}=\vec{k}_z+\vec{q}$, where $\vec{\rho}$ and $\vec{q}$ are two-dimensional vectors. Then,

$$\begin{aligned} I = -16\pi^2\Bigg[\int \delta(E+\vec{Q}\cdot\vec{v})\exp(i\vec{Q}\cdot\vec{p})A^{-1-i\alpha_p} \\ \times(A-B)^{i\alpha_p} C^{-1-i\alpha_T}(C-D)^{i\alpha_T} d\vec{Q}\Bigg]. \end{aligned} \tag{12}$$

The integration over $\vec{Q}_z$ can easily be performed using the property of the δ function, and finally we are left with a two-dimensional integral over $\vec{\rho}$.

Following the work of Ref. [9], we may finally write the transition amplitude as

$$c_k(p) = -16\pi^2 A_k \int \exp(i\vec{p}\cdot\vec{\rho})F(\vec{\rho})d^2\vec{\rho}, \tag{13}$$

where A_k is constant and

$$F(\vec{\rho})=c_1 f_1(\vec{\rho}) f_1'(\vec{\rho})+c_2 f_2(\vec{\rho}) f_2'(\vec{\rho})+\cdots + c_{n-1} f_{n-1}(\vec{\rho}) f_{n-1}'(\vec{\rho})+c_n f_n(\vec{\rho}) f_n'(\vec{\rho}), \quad (14)$$

with $c_1, c_2, \ldots, c_n$ as the coefficients of Slater orbitals.

The above expression is a linear combination of amplitudes that comes through the bound-state wave function that is a linear combination of Slater-type orbitals (STO's). In the expression (14),

$$f_1(\vec{\rho})=[\phi_1]^{-1-i\alpha_p}[\phi_2]^{i\alpha_p}[\phi_{31}]^{-2-i\alpha_T}[\phi_{41}]^{-1+i\alpha_T},$$

$$f_1'(\vec{\rho})=(2\alpha_T k_T-2\beta_1)\phi_{31}+2\beta_1(L+k_T^2-2\beta_1\alpha_T k_T) + i2\beta_1(\alpha_T L+\alpha_T k_T^2+2\beta_1 k_T),$$

$$f_2(\vec{\rho})=[\phi_1]^{-1-i\alpha_p}[\phi_2]^{i\alpha_p}[\phi_{32}]^{-2-i\alpha_T}[\phi_{42}]^{-1+i\alpha_T},$$

$$f_2'(\vec{\rho})=(2\alpha_T k_T-2\beta_2)\phi_{32}+2\beta_2(L+k_T^2-2\beta_2\alpha_T k_T) + i2\beta_2(\alpha_T L+\alpha_T k_T^2+2\beta_2 k_T).$$

Similarly, we can write

$$f_n(\vec{\rho})=[\phi_1]^{-1-i\alpha_p}[\phi_2]^{i\alpha_p}[\phi_{3n}]^{-2-i\alpha_T}[\phi_{4n}]^{-1+i\alpha_T},$$

$$f_1'(\vec{\rho})=(2\alpha_T k_T-2\beta_n)\phi_{3n}+2\beta_n(L+k_T^2-2\beta_n\alpha_T k_T) + i2\beta_n(\alpha_T L+\alpha_T k_T^2+2\beta_n k_T),$$

where

$$\phi_1=\left(\vec{\rho}-\frac{\vec{q}}{2}\right)^2+a^2,$$

$$\phi_2=\rho^2+A_1-i\eta \quad (\eta\to 0),$$

$$\phi_{31}=\left(\vec{\rho}+\frac{\vec{q}}{2}\right)^2+s_1^2, \quad \phi_{41}=\left(\vec{\rho}-\frac{\vec{q}}{2}\right)^2+B_1,$$

$$\phi_{32}=\left(\vec{\rho}+\frac{\vec{q}}{2}\right)^2+s_2^2, \quad \phi_{3n}=\left(\vec{\rho}+\frac{\vec{q}}{2}\right)^2+s_n^2,$$

$$\phi_{42}=\left(\vec{\rho}-\frac{\vec{q}}{2}\right)^2+B_2, \quad \phi_{4n}=\left(\vec{\rho}-\frac{\vec{q}}{2}\right)^2+B_n,$$

$$a^2=|\vec{Q}_z-\vec{v}/4-\vec{k}_z/2|^2,$$

$$A_1=A_2+\vec{q}\cdot\vec{\rho},$$

$$A_2=Q_z^2-3\left(\frac{q^2+k_z^2}{4}\right)+5\frac{v^2}{16}+\vec{k}_z\cdot\frac{\vec{v}}{4}-3\vec{Q}_z\cdot\frac{\vec{v}}{2}+Q_z k_z,$$

$$B_1=a^2+(\beta_1-ik_T)^2,$$

$$B_2=a^2+(\beta_2-ik_T)^2,$$

$$B_n=a^2+(\beta_n-ik_T)^2,$$

$$y^2=|Q_z+v/4+k_z/2|^2,$$

$$L=2\left[Q_z\left(k_z+\frac{v}{2}\right)+\vec{\rho}\cdot\vec{q}\right],$$

$$s_1^2=y^2+\beta_1^2, \quad s_2^2=y^2+\beta_2^2, \quad s_n^2=y^2+\beta_n^2.$$

It may be observed that only the terms $\phi_{31}\ldots\phi_{3n}$ and $\phi_{41}\ldots\phi_{4n}$ depend on the exponents β_j of the Slater orbitals and are different for each individual amplitude. Care must be taken with the cross terms like $f_1^*(\vec{\rho})f_1'^*(\vec{\rho})f_2(\vec{\rho})f_2'(\vec{\rho})$ in the ionization probability.

Again, in the evaluation of the ionization probability, special attention must be given to the factors $\phi_{41}\ldots\phi_{4n}$, as there exists a negative imaginary part, and the corresponding phase factor arising due to these should be properly accounted for. Detailed discussions regarding this have been made in the previous work [9].

Now the total ionization cross section can be written as

$$\sigma_{\text{total}}=2\pi\int\frac{d^2\sigma}{dE_e d\Omega_e}\sin\theta_e d\theta_e dE_e,$$

where

$$\frac{d^2\sigma}{dE_e d\Omega_e}\approx k\int dp|c_k(p)|^2$$

is the doubly differential ionization cross section (DDCS). (The symbols have their usual meaning.)

III. RESULTS AND DISCUSSIONS

In the present article, we have studied the following reactions:

$$p,p^-+Y\to p,p^-+Y^+ +e^-, \quad (15a)$$

$$X^{Z+}+Y\to X^{Z+}+Y^+ +e^-. \quad (15b)$$

In the reactions (15a) and (15b), Y denotes the one-electron target of He and Li and in reaction (15b), X^{Z+} denotes the bare nuclei of He, Li, Be, B, C, N, O, F, and Ne. Z is the corresponding nuclear charge.

A. Total ionization cross section

Total ionization cross sections (TICS's) are obtained from the doubly differential cross-section (DDCS) values simply by numerical integration over the angles and the ejected energies. Although much information regarding the mechanism of the reaction cannot be obtained from TICS's, they are still useful because they provide information about the quality of the theoretical approach when compared with the experimental data.

In Fig. 1, we present the total ionization cross sections for the single ionization of He by impact of multiply charged ions such as He^{2+} and Li^{3+}. For comparison, we also plot the experimental results of Shah and Gilbody [18], Shah *et al.* [19], and Knudsen *et al.* [26], as well as the existing

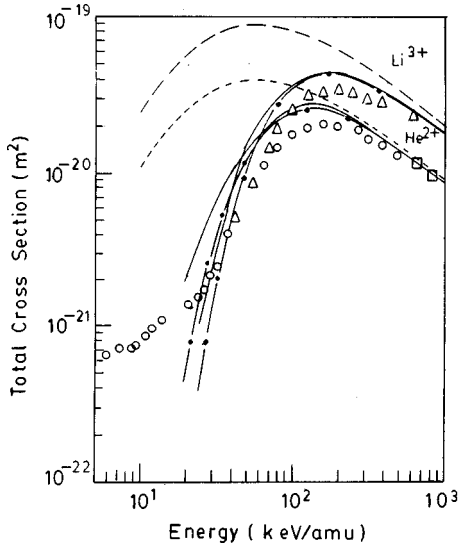

FIG. 1. Total ionization cross section of He by He^{2+} and Li^{3+} impact as a function of collision energy. Present results: (——) for He^{2+} and (——) for Li^{3+}; CDW-EIS (—·—); Born: (– – –); experimental data, Ref. [18] (○○○), and Ref. [19] (□□□) for He^{2+}; Ref. [26]; (△△) for Li^{3+}.

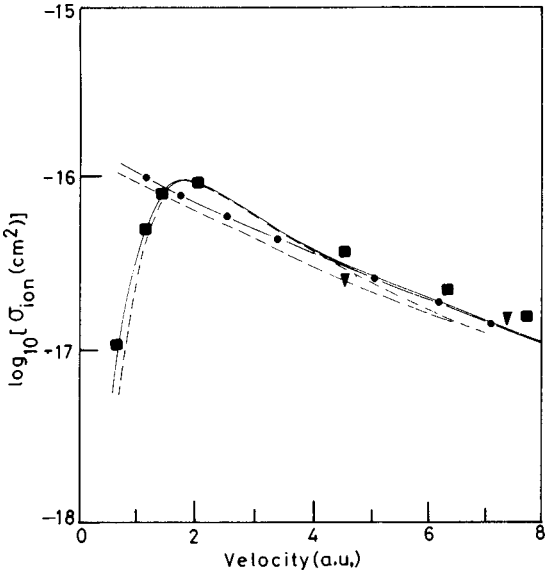

FIG. 2. Total ionization cross section for the single ionization of helium by proton and antiproton impact. Present results for protons (——); for antiprotons: (—·—); experimental data, Ref. [16]: (■■) for protons and Ref. [28]; (▼▼) for antiprotons, CTMC; (----) for protons and (––) for antiprotons.

theoretical values. The present results for He^{2+} and Li^{3+} impact ionization show good accord with the predictions of other theories and the experimental data at intermediate and high energies. However, in the low-impact energy region the present results, along with other theoretical models such as the FBA and CDW-EIS [27] for He^{2+} and Li^{3+} impact, fail to reproduce the experimental data, but the CDW-EIS and present results agree much better than do the FBA results. The discrepancy with experiment in the low-energy region may be attributed to the fact that coupling with other channels becomes important there.

In Fig. 2, we compare the present values for the ionization of He by proton and antiproton impact in the velocity range 1–8 a.u. with the results of the classical trajectory Monte Carlo (CTMC) method (Schultz *et al.* [7]) and the experimental data of Rudd *et al.* [16] for proton impact and of Andersen *et al.* [28] for antiproton impact. Our values are found to be in fairly good agreement with the experimental data for both proton and antiproton impact. At the higher impact velocities, the present results both for proton and antiproton impact are found to be smaller in magnitude than the experimental data but larger than the results obtained by CTMC calculations. The antiproton cross sections are higher in magnitude than the proton cross sections at the lower impact velocities. Comparison between the proton and antiproton impact cross sections is of considerable interest because for negatively charged projectiles there is no charge-transfer channel. It can be seen from the figure that at higher energies proton and antiproton cross-section values are same, while there is a marked difference in the low- and intermediate-impact velocity region. The FBA predicts equal cross-section (not shown) values for both projectiles independent of impact energies.

In Fig. 3, the single-ionization cross sections for proton and antiproton impact of Li $(1s)$ are presented. These values are compared with the experimental data of Shah *et al.* [29] as well as the CDW-EIS results of McCartney and Crothers [13]. The present results agree with the experimental data of Ref. [29] for proton impact in the energy range above 600 keV. However, our findings are somewhat higher than the values of McCartney and Crothers [13] for both proton and antiproton impact throughout the energy region considered.

Figure 4 presents the total ionization cross sections of Li from the $1s$ subshell by impact of multiply charged bare ions ranging from He^{2+} to Ne^{10+}. The present values for He^{2+} impact are found to be in good agreement with the data of Shah *et al.* [29] throughout the energy region considered. The values calculated by using the CDW-EIS [13] somewhat underestimate the present results. For other multiply charged

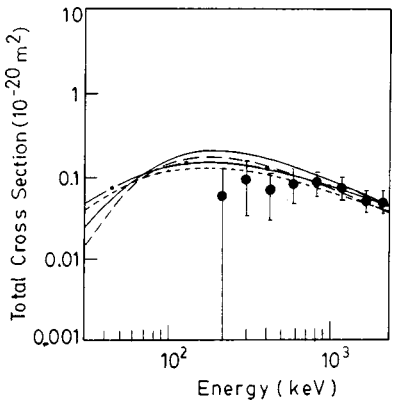

FIG. 3. Total ionization cross section for the single ionization of Li $(1s)$ by proton and antiproton impact. Present results: (——) for protons and (—·—) for antiprotons. CDW-EIS: Ref. [13], (----) for protons and (–––) for antiprotons; experimental data, Ref. [29]: (●●●) for protons.

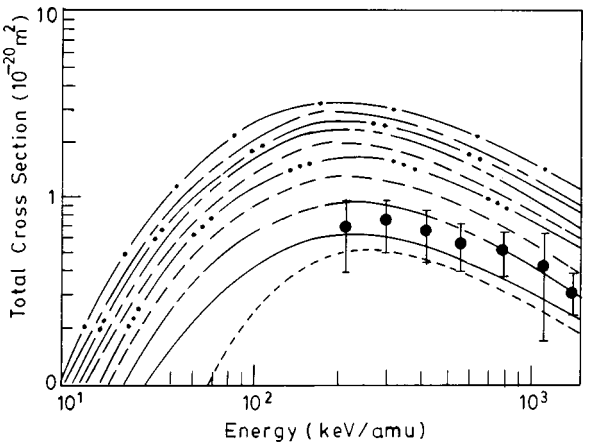

FIG. 4. Total ionization cross section of Li$(1s)$ by the impact of He^{2+}, Li^{3+}, Be^{4+}, B^{5+}, C^{6+}, N^{7+}, O^{8+}, F^{9+}, and Ne^{10+} as a function of collision energy. Present results: (——) for He^{2+}, (— - - —) for Li^{3+}, (- -) for Be^{4+}, (—··—) for B^{5+}, (--) for C^{6+}, (— — —) for N^{7+}, (—··–) for O^{8+}, (— - —) for F^{9+}, and (—·—) for Ne^{10+}. CDW-EIS Ref. [13], for He^{2+}, (----); experimental data, Ref. [29], (●●●) for He^{2+}.

bare ions impacting on Li atoms, the present results are found to be qualitatively the same as for α-particle impact. The cross-section values, however, increase with ionic charge.

B. Differential ionization cross section

In the last few years, much effort has been put forth to study and understand the single-ionization processes in ion-atom collisions both theoretically and experimentally. Since in the postcollisional regime the electron moves in a double continuum of both the projectile and the residual target atom, it is necessary to understand the momentum distribution of

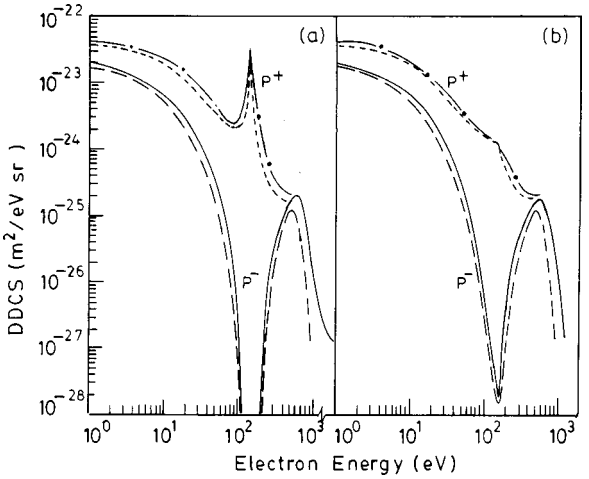

FIG. 5. DDCS for ionization of He by 300-keV proton and antiproton impact for ejection angles of (a) 0° and (b) 10° (a) Present results: (—·—) for protons and (——) for antiprotons. CDW-EIS: Ref. [30], (----) for protons, (– – –) for antiprotons. (b) Present results: (—·—) for protons and (——) antiprotons; CDW-EIS: Ref. [30], (----) for protons and (– – –) for antiprotons.

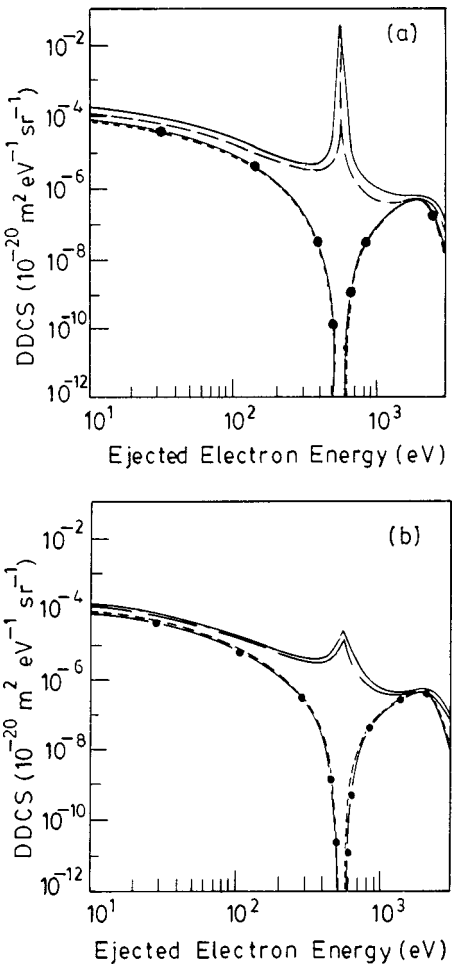

FIG. 6. DDCS for ionization of Li by 1-MeV proton and antiproton impact for ejection angles of (a) 0° and (b) 1°. (a) Present results: (——) for protons and (—·—) for antiprotons. CDW-EIS: Ref. [13], (– –) for protons, (----) for antiprotons. (b) Present result: (——) for protons and (----) antiprotons; CDW-EIS. Ref. [13], (– –) for protons and (—·—) for antiprotons.

the ejected electron clearly. It has been well established from the study of differential cross sections that the electron ejected spectra is rich in different kinds of structures, such as the electron capture to continuum (ECC) peak, binary encounter peak, and exponential dip (for negatively charged projectile), in the ionization of monovalent target atoms such as hydrogen. Calculation of the differential cross sections has a similar importance for the study of these features in the case of the ionization of multielectronic target atoms by the impact of bare ions of highly charged nuclei.

C. Doubly differential cross section

Figures 5(a) and 5(b) display the doubly differential cross sections for 300-keV proton and antiproton impact on He at 0° and 10°, respectively, as a function of ejected energy. Comparison has been made with the theoretical results of Fainstein *et al.* [30] calculated using the CDW-EIS model. The present perturbative approach calculates values of slightly higher magnitude but displays the position of the ECC peak for proton and the exponential dip for antiproton

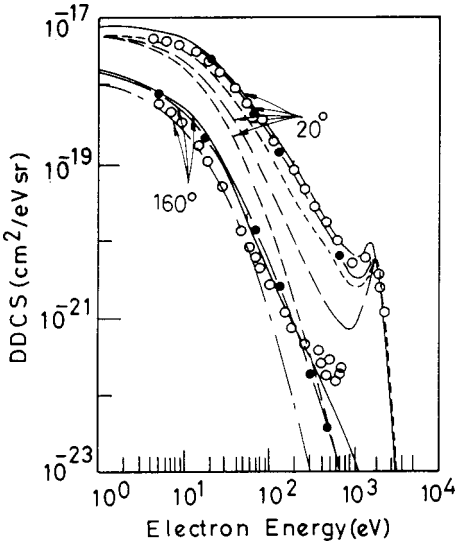

FIG. 7. DDCS for ionization of He by 1-MeV/amu O^{8+} impact for fixed ejection angles of 20° and 160°. Present results: (——); CDW-EIS: Ref. [20], (----); CDW: Ref. [20], (—·—); Born: Ref. [20], (– – –); experimental data: Ref. [31], (○○○).

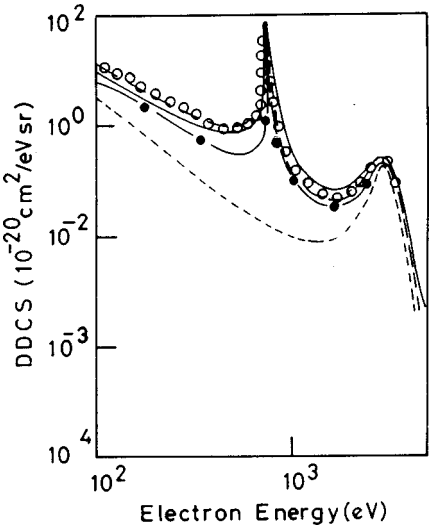

FIG. 8. DDCS for ionization of He by 1-MeV/amu F^{9+} impact. Present results: (——); CDW-EIS. Ref. [20], (—·—); CDW: Ref. [20], (––); Born: Ref. [20], (----); experimental data: Ref. [32], (○○○).

impact, in exact agreement with the prediction of the CDW-EIS model. From Fig. 5(b), it is evident that at the ejection angle of 10° in the case of proton impact, the peak reduces to only a small hump in comparison with the prominent peak at 0°. The dip due to antiproton impact, however, persists to 10° ejection angles.

In Figs. 6(a) and 6(b), we display the present calculated results for 1-MeV proton and antiproton impact on Li at fixed ejection angles of 0° and 1°, respectively. As in the case of proton and antiproton impact on He, the present results show similar structures as predicted by the CDW-EIS model of McCartney and Crothers [13]. Our results are slightly greater than the CDW-EIS values throughout the ejection energy range.

For the case of multiply charged ion impact, we display in Fig. 7 our present doubly differential cross-section values by O^{8+} impact on He at 1 MeV/amu. The DDCS is plotted as a function of electron ejection energy at fixed emission angles of 20° and 160°. In the same figure, the results of the FBA, CDW, and CDW-EIS [20] as well as the experimental data of Pedersen *et al.* [31] are shown. The present cross section values at 20° are closer to the experimental data as well as to the results of recent CDW calculations, but are higher than the theoretical values calculated by using the FBA and CDW-EIS. For the ejection angle of 160°, the present results along with the results of the CDW overestimate the experimental data and the values of the FBA and CDW-EIS in the ejection energy range 1–150 eV. The present results at 160° markedly deviate from the values at an ejection energy of about 300 eV.

In Fig. 8, we present the DDCS as a function of the ejection energy by the impact of 1-MeV/amu F^{9+} on He. For comparison, we also include the recent results of Gulyas and Fainstein [20] and McCartney and Crothers [13], calculated by using the FBA, CDW-EIS and CDW, along with the experimental data of Lee *et al.* [32]. The present values, along with the CDW and CDW-EIS, reproduce the experimental ECC peak, though at the low ejection energies, the present approach gives values of smaller magnitude, where the FBA fails to produce the ECC peak. As this feature occurs due to the two-center effect, the FBA could not account for this effect since the ejected electron in the final state is considered to be moving in the continuum of the target nucleus alone. The other theories, including the present one, consider the distortions in the final state due to both the projectile and the residual target to be on equal footing.

Figures 9(a) and 9(b) display the angular distributions of the ejected electrons for 150- and 1000 eV ejected energies

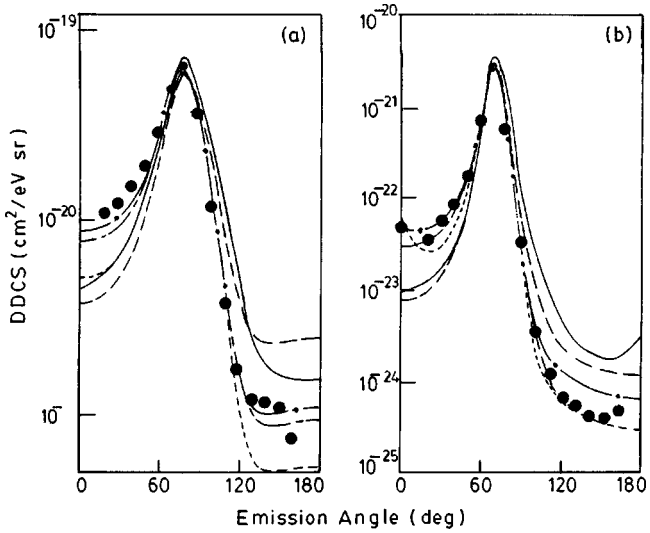

FIG. 9. DDCS of He by 5-MeV/amu Ne^{10+} impact as a function of ejection angles for fixed ejection energy of (a) 150 eV and (b) 1000 eV. Present results: (——); CDW: Ref. [20], (—·—); CDW-EIS: Ref. [20], (— - —); Born: Ref. [20], (––); Ref. [15], (----), experimental data: Ref. [33], (●●●).

by the impact of 5-MeV/amu Ne^{10+} on He, respectively. We also present the values of Gulyas and Fainstein [20], calculated using the CDW, FBA, and CDW-EIS, as well as the experimental measurements of Stolterfoht *et al.* [33]. The present calculated values show fairly good agreement with experiment and the other theories at smaller angles, but at larger angles the present values are of higher magnitude. This disagreement at larger angles may be due to the improper description of the continuum orbitals. Theoretical calculations for angular distributions of ejected electrons are very sensitive to the description of continuum orbitals [15]. Gulyas and Fainstein have used numerical wave functions and have found improvements in their results.

IV. CONCLUSION

In this article, we present the results of total and differential ionization cross sections of multielectron targets such as He and Li by the impact of protons, antiprotons, and fully stripped bare ions. The active electron is assumed to move under the influence of an effective potential due to the passive electron(s) and the target core. Slater-type orbitals are used for the initial bound state of the target atoms. The results thus obtained are found to be encouraging since they agree well with the experimental data as well as with the values of the recently developed CDW-EIS and CDW models for multielectron targets in the high-impact energy range. The present approach is also suitable for studying the various features of ionization spectra since the final electronic state considers the distortion due to the projectile and the residual target ions on an equal footing. However, in the low-energy region it fails to estimate correct results. The present perturbative approach is easier to tackle numerically than the other approaches and predicts reasonably good results in the intermediate and high energies.

ACKNOWLEDGMENTS

The authors would like to express their thanks to Dr. C. R. Mandal, Dr. M. Das, and M. Purkait for stimulating discussions. Financial support from the International Atomic Energy Agency (IAEA), Vienna, is gratefully acknowledged.

[1] A. Salin, J. Phys. B **21**, 631 (1969).
[2] Dz. Belkic, J. Phys. B **11**, 3529 (1978).
[3] H. A. Bethe, Ann. Phys. (N.Y.) **5**, 325 (1930).
[4] H. S. W. Massey and C. B. O. Mohr, Proc. R. Soc. London, Ser. A **140**, 613 (1933).
[5] D. R. Bates and G. Griffing, Proc. Phys. Soc., London, Sect. A **66**, 961 (1953).
[6] N. Stolterfoht, R. D. Dubois, and R. D. Rivarola, *Electron Emission in Heavy Ion Atom Collision* (Springer, Berlin, 1997).
[7] D. R. Schultz, R. E. Olson, C. O. Reinhold, M. W. Gealy, G. W. Kerby III, Y. Y. Hsu, and M. E. Rudd, J. Phys. B **24**, L599 (1991).
[8] D. S. F. Crothers and J. F. McCann, J. Phys. B **16**, 3229 (1983).
[9] S. Sahoo, K. Roy, N. C. Sil, and S. C. Mukherjee, Phys. Scr. **58**, 126 (1998).
[10] N. Toshima, Phys. Rev. A **50**, 3940 (1994).
[11] S. Sahoo, K. Roy, N. C. Sil, and S. C. Mukherjee, Indian J. Pure Appl. Phys. **37**, 460 (1999).
[12] P. D. Fainstein, V. H. Ponce, and R. D. Rivarola, J. Phys. B **21**, 287 (1988); P. D. Fainstein and R. D. Rivarola, Phys. Lett. A **150**, 23 (1990).
[13] M. McCartney and D. S. F. Crothers, J. Phys. B **26**, 4561 (1993).
[14] E. Clementi and C. Roetti, At. Data Nucl. Data Tables **14**, 177 (1974).
[15] L. Gulyas, P. D. Fainstein, and A. Salin, J. Phys. B **28**, 245 (1995).
[16] M. E. Rudd, Y. K. Kim, D. H. Madison, and J. W. Gallagher, Rev. Mod. Phys. **57**, 965 (1985).
[17] D. H. Madison, Phys. Rev. A **8**, 2449 (1973).
[18] M. B. Shah and H. B. Gilbody, J. Phys. B **18**, 899 (1985).
[19] M. B. Shah, P. McCallion, and H. B. Gilbody, J. Phys. B **22**, 3037 (1989).
[20] L. Gulyas and P. D. Fainstein, J. Phys. B **31**, 3297 (1998).
[21] D. S. F. Crothers, J. Phys. B **15**, 2061 (1982).
[22] A. M. Ermolaev, C. J. Noble, and B. H. Bransden, J. Phys. B **15**, 457 (1982).
[23] A. M. Ermolaev, J. Phys. B **17**, 1069 (1984).
[24] R. Shingal, B. H. Bransden, A. M. Ermolaev, D. R. Flower, C. W. Newby, and C. J. Noble, J. Phys. B **19**, 309 (1986).
[25] A. Nordsieck, Phys. Rev. **93**, 785 (1954).
[26] H. Knudsen, L. H. Andersen, P. Hvelplund, G. Astner, K. Cederquist, H. Danared, L. Liljeby, and K.-G. Rensfelt, J. Phys. B **17**, 3545 (1984).
[27] P. D. Fainstein, V. H. Ponce, and R. D. Rivarola, Phys. Rev. A **36**, 3639 (1987).
[28] L. H. Andersen, P. Hvelplund, H. Knudsen, S. P. Moller, K.-G. Rensfelt, and E. Uggerhoj, Phys. Rev. Lett. **57**, 2147 (1986).
[29] M. B. Shah, D. S. Elliot, and H. B. Gilbody, J. Phys. B **18**, 4245 (1985).
[30] P. D. Fainstein, V. H. Ponce, and R. D. Rivarola, J. Phys. B **21**, 2989 (1988).
[31] J. O. P. Pedersen, P. Hvelplund, A. G. Petersen, and P. D. Fainstein, J. Phys. B **23**, L597 (1990); **24**, 4001 (1991).
[32] D. H. Lee, P. Richard, T. J. M. Zouros, J. M. Senders, J. M. Shinpaugh, and H. Hidmi, Phys. Rev. A **24**, 97 (1990).
[33] N. Stolterfoht, H. Platten, G. Schiwietz, D. Schneider, L. Gulyas, P. D. Fainstein, and A. Salin, Phys. Rev. A **52**, 3796 (1995).